In vitro imaging of the carotid artery with spatial compound imaging

空間的加算映像法を用いた in vitro における頸動脈断層像の計測

Jens E. Wilhjelm,[1] Søren K. Jespersen,[2] Jon U. Hansen,[1] Talo Brandt,[1] Kim Gammelmark[1] and Henrik Sillesen[3]

Center for Arteriosclerosis Detection with Ultrasound (CADUS)
E-mail: wilhjelm@it.dtu.dk. Homepage: www.it.dtu.dk/~wilhjelm/cadus. FAX: +45 4588-0117.

[1]Dept. of Information Tech., Technical University of Denmark, Bldg. 344, DK-2800 Lyngby, Denmark.

[2]B-K Medical A/S, Sandtoften 9, DK-2820 Gentofte, Denmark,

[3]Dept. of Vascular Surgery, Gentofte University Hospital, DK-2900 Hellerup, Denmark.

With the aim of investigating possible improvements in visualization of carotid atherosclerotic plaque, a new dedicated off-line multi-angle ultrasound compound scanner has been built and tested on human tissues. Images were recorded from 7 insonification angles over a range of 42 degrees and the individual single-angle images were combined (averaged) into a single image (spatial compounding). This technique is denoted multi-angle compound imaging (MACI). Compared to conventional B-mode imaging, this method features less angle-dependent images, since more scan lines are perpendicular (or nearly perpendicular) to the tissue interfaces. Further, the spatial compounding strongly diminishes the speckle pattern. These improvements are illustrated with *in vitro* images of human atherosclerotic plaque.

spatial compound imaging, atherosclerotic plaque, linear array, speckle reduction

1 . Introduction

The existence of atherosclerotic plaque in the carotid arteries increases the risk of stroke, however surgical removal of the plaque has proven beneficial in reducing this risk.[1] Unfortunately, ultrasonic assessment of size, shape and type of the lesions is often seriously limited by poor visualization of the artery wall and plaque. Some of the reasons for this are: *i)* Certain plaque materials, such as certain lipids, are echolucent in nature[4] and will always be difficult to visualize. *ii)* Other non-isotropic materials, such a fibrous tissues or the vessel wall itself, produce echo signals with a strong angle-dependence[4] resulting in fluctuations in echogenicity with rotation and movement of the transducer. *iii)* Because the pathological thickening of the intima in the carotid wall is rarely more than 4 mm, the region of interest on the ultrasound image is only some 20 wavelengths thick (assuming a transducer frequency of 7.5 MHz and a mean sound speed of 1540 m/s). Due to the speckle noise present in this small ultrasound image region, residual lumen, plaque outline and plaque type (hard or soft type of plaque) can often be difficult to assess.

A possible way to solve some of these problems is to use spatial compound imaging with which the angle-dependence and the speckle noise can be reduced[6, 7]. For this reason, a digital off-line ultrasound scanner for multi-angle compound imaging (MACI) was build with the purpose of improving visualization of vascular tissue. This paper describes the instrument and the *in vitro* results obtained when scanning formalin fixed human atherosclerotic plaque molded into an agar block for fixation.

2 . Principle of Operation

The MACI system makes use of a conventional low-pitch linear array transducer with 192 transducer elements. The active aperture is selected as a subset of the 192 elements and this aperture is then operated in phased array mode, to create a beam with a given angle. This angle is denoted θ_i. The aperture is then moved electronically along the entire array to record a complete image at that specific angle. This operation is repeated for all beam angles, θ_i, where $i = 1, 2, ..., N_\theta$. Figure 1 illustrates some of the scan lines used in this procedure when $N_\theta = 3$. In Figure 1 and in this work, the angles are chosen symmetrically around 0˚. It is seen that the fully compounded region has a triangular shape. From the geometry on Figure 1, the depth of this region can be found to:

$$z_{max}(D, \theta_{max}) = \frac{D}{2\tan(\theta_{max})} \quad (1)$$

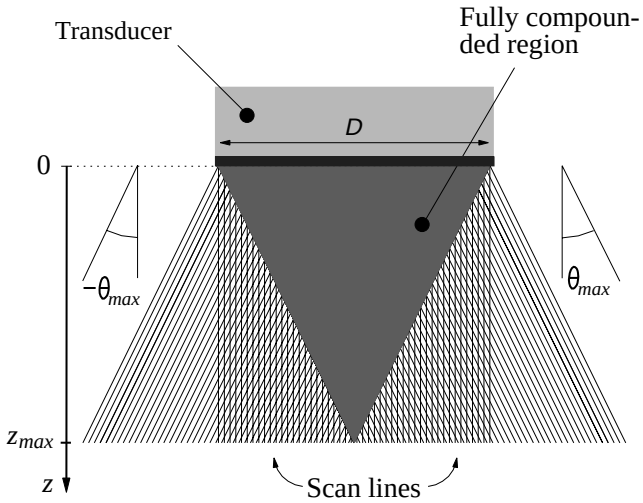

Figure 1 Illustration of scan lines and angles for the recording of three single-angle images used in creating the multi-angle compound image.

where D is the total array length and θ_{max} is the largest beam angle. As an example, consider $D = 40$ mm and $\theta_{max} = 21$˚, which gives $z_{max} = 52.1$ mm.

3 . System Hardware

The system hardware is outlined in Figure 2. It consist of three major components: *i)* A 192-element linear transducer array (LA/7.5/192/HD, Vermon, Tours, France) with a center frequency of 7.5 MHz and a pitch equal to 208 μm. The array length is $D = 40$ mm. *ii)* A control workstation containing a PCI-based 12 bit AD-card (CompuScope 6012/PCI, GaGe Applied Sciences, Montréal, Québec, Canada) and a timing controller (Real-time scan controller, RTSC) for controlling the ultrasound system. *iii)* A 19" rack containing the transmit and receive system hardware, power supply and transducer connector.

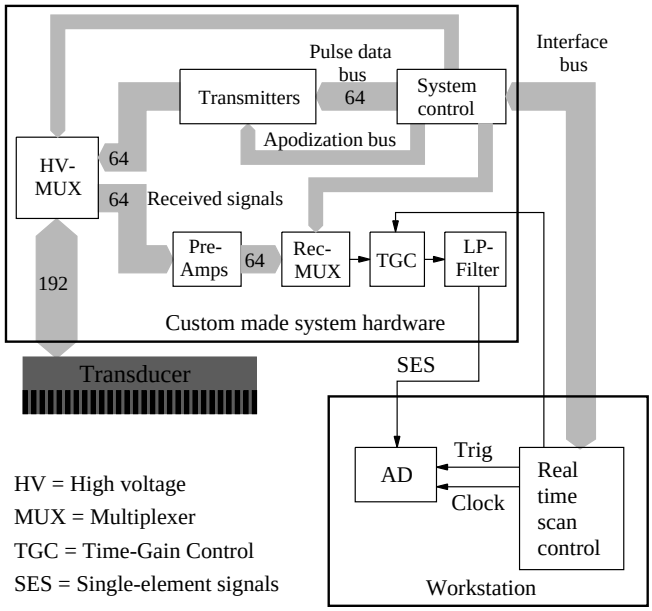

Figure 2 Block diagram of system components.

The real-time transmit system contains 64 parallel transmitters with fully programmable transmit delays (in the range 0 - 34 μs) and apodization control (in the range –25 - 0 dB). The delay resolution of the transmit system is 16.7 ns. The receiver system consist of 64 parallel pre-amplifiers and a multiplexer which selects *one* of the receive channels at a time (thus the single-element signals are recorded one by one). This one signal is next passed through a time-gain control (TGC) amplifier and an anti-aliasing lowpass filter before digitalization in the 12 bit AD-converter. In this study, the signals are digitized with a sampling frequency of 40 MHz (it can be a high as 60 MHz).

All clock signals (including ADC clock), timing signals, TGC voltage, *etc.*, are generated by the RTSC board which is mounted in the control workstation. This approach yields very low jitter between recorded single-element signals, which is crucial when sampling the single-element signals one at a time and beamforming off-line. Typical recording time for a single image (192 scan lines each of 64 single element signals) is two to three minutes.

4 . Signal Processing in Software

The system software consists of three main parts: *i)* Creation of setup data for the entire system, *ii)* Control of the transmit and receive hardware as well as recording of the single element signals and *iii)* processing of the received single-element signals for generation of images.

The setup data is created with a Matlab user interface, while the remaining software is written in C language in order to form a complete stand-alone program that can run the entire recording process including display of the recorded images. Data can be saved at all levels of the signal processing sequence making it very well suited for research purposes.

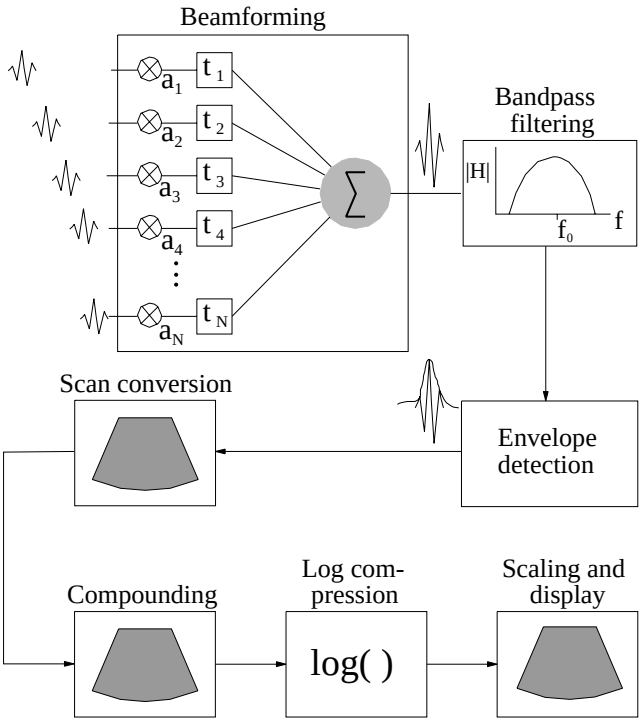

Figure 3 Block diagram of signal processing made in software.

The elements of the digital signal processing performed on the received signals are shown in Figure 3 and consist of dynamic beamforming, bandpass filtering, envelope detection and scan conversion. As the sensitivity of the individual elements of the ultrasound transducer varies with angle, this is compensated as part of the scan conversion, in order to provide the same sensitivity for all angles. The compound image is generated by averaging the single-angle images, however, it is only in the fully compounded region that all single-angle images contribute to this averaging. The last part of the signal processing consist of logarithmization, scaling and display.

5 . Resolution size and Speckle

The size of the point spread function was measured with a point scatterer phantom[2] consisting of a single ~100 μm diameter glass sphere molded into the center of an agar block. The glass sphere was located ~35 mm from the transducer. Images were recorded from 11 different angles in steps of 5˚. The −6 dB width of the point spread function measured from the 0˚ image in the lateral and axial directions, was 0.7 mm and 0.21 mm, respectively. The same measures for the compound image were 0.77 mm and 0.27 mm, respectively. Thus, at this depth, the spatial compounding increase the point spread function by ~30 %.

Speckle reduction was investigated experimentally.[3] In comparison to conventional imaging, the signal-to-noise ratio was increased by a factor of 2.4 and 2.6 when using 6 angles separated 10˚ and 11 angles separated 5˚, respectively. These results are in excellent agreement with theory[5].

6 . Tissue Preparation

Formalin fixed carotid atherosclerotic plaques removed during prophylactic carotid endarterectomy were molded into a rectangular agar block. By supporting the plaque on tiny wires during molding, the plaque was made floating inside the agar block. A lid with two bands of small rectangular openings was placed on the liquid agar. When the liquid agar had hardened, the upper surface of the agar block then contained two bands of index markers, both running parallel with the "long axis" of the plaque. These index markers were visible on the ultrasound images and they were also used for slicing the plaque after scanning. Figure 4 provides an illustration of the agar block as seen from the transducer. The two bands of markers were located so that they were at the extreme sides of the ultrasound images, in order to avoid variation in the interference on the echo signals from the plaque due to the water-agar interface.

The distance between two adjacent markers, Δy_h, was 5 mm. Slicing was done both at the center of a marker ("peak") and between two markers ("valley"). Thus the distance between slices was 2.5 mm. After cutting each slice, a macroscopic photograph was taken of the slice. There were typically 8 to 16 slices per plaque.

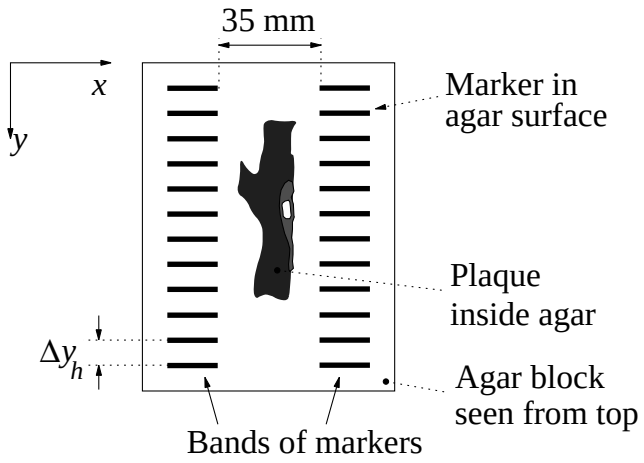

Figure 4 Illustration of the components of the agar block, as seen from the top (= as seen from the transducer). The plaque is completely inside agar, while the agar markers are located on the top of the block. The drawing is not to scale.

7 . Results

Ultrasound images were recorded at parallel cross-sectional scan planes covering the entire plaque. The separation between scan planes was 0.5 mm. Seven single-angle images were recorded at each scan plane using the angles −21˚, −14˚, −7˚, 0˚, 7˚, 14˚ and 21˚. The conventional B-mode image corresponds to the 0˚ image, while the MACI image was obtained from averaging of all seven single-angle images. The scanning took place in pure demineralized water at ~20˚.

The markers on the agar surface was identified from the appropriate region on the 0˚ image. By exactly identifying which ultrasound scan plane that corresponded to a given slice, a unique relationship between ultrasound images and anatomical macroscopic photos was obtained.

Typical ultrasound images are provided in Figure 5a and b, which shows a 400x400 pixel (20x20 mm) region centered at a depth of 25 mm. Figure 5c shows the corresponding macroscopic photograph with metric axes.

The images show plaque from the internal carotid artery surrounded by the intima layer and possible some part of the media layer. The

opening towards the top of the image, is the surgical cut made during the removal of the plaque.

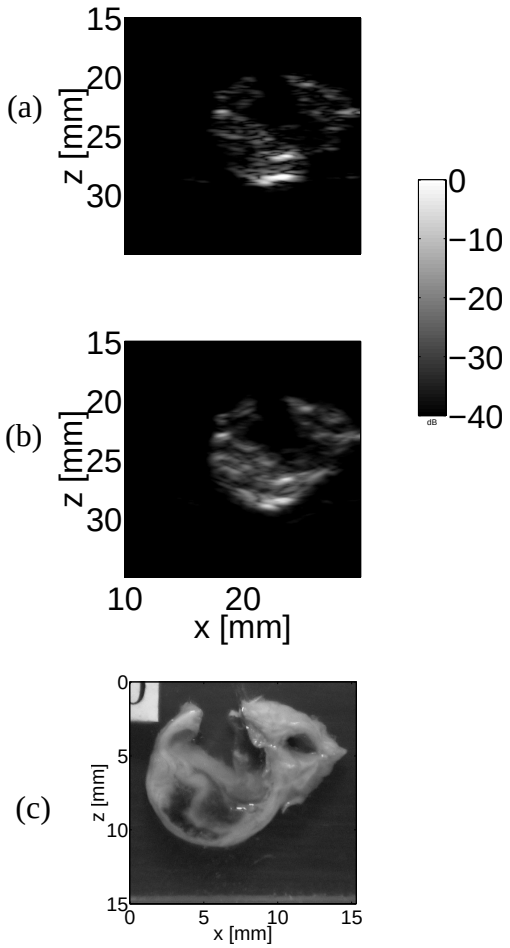

Figure 5 (a) conventional and (b) compound cross-sectional images of atherosclerotic plaque. (c) macroscopic photograph taken at the same plane as the ultrasound image. The photograph was taken during slicing of the plaque.

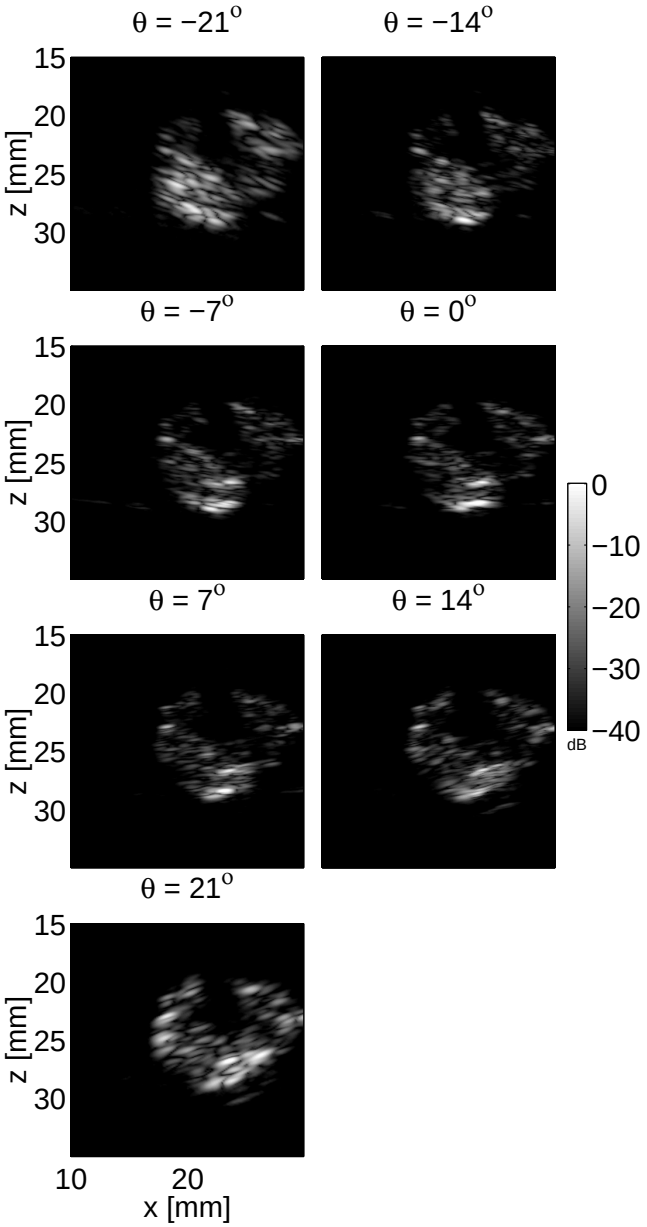

Figure 6 The seven single-angle images used to create the compound image in Figure 5a.

In order to further study the angle-dependence, Figure 6 shows the individual single-angles images used to produce Figure 5b. Notice the rather poor definition of the outline in the single-angle images, compared to the corresponding compound image in Figure 5b.

8 . Discussion

The results in Figures 5 show improved visualization of boundaries. This is partly due to the fact that more scan lines are perpendicular or nearly perpendicular to the reflecting surfaces (e.g. intima layers), partly due to the reduced speckle noise. When comparing the compound image in Figure 5b to the anatomical image in Figure 5c, it is seen that there is some deviation. There can be several reasons for this:

a) When the plaque was sliced, great care was taken to avoid displacing the individual plaque fragments, relative to each other. Nevertheless, displacement of some parts of the plaque was unavoidable.

b) In some regions, where the anatomical image is free from plaque, the ultrasound image might not be completely black. This might be due to grating-lobes effects.

c) Finally, each scan line was subjected to the same TGC. This is slightly wrong, as the scanning was done in pure water, with no attenuation. Ideally, the TGC curve should only be applied to the part of the received signals that originates from plaque. (This will be implemented in future investigations).

When considering the single-angle images in Figure 6, it is seen that there is some difference between which areas of the plaque, that is "picked-up" by the ultrasound imaging technique. Comparing the angles $\theta = \pm 21^{\circ}$, differences are seen in the three to six o'clock direction. On the other hand, the region at about one o'clock is rather equally imaged, at all angles.

Despite the encouraging results arrived at in this investigation, it should be noted that a number of factors may influence the achievable image quality *in vivo*. Two of these are based on the fact that single images are recorded and then added:[3] a) spatial variation in the speed of sound which might cause blurring in the MACI image, due to misalignment between the individual single-angle images and b) tissue movement might also cause some image blurring (if the individual single-angle images are recorded consecutively, these might not align completely when added to form the compound image).

9 . Conclusions

A new imaging modality, Multi-Angle Compound Imaging, has been described and *in vitro* results based on formalin fixed human atherosclerotic plaque molded into agar have been presented. The results showed that the MACI image features reduced speckle noise and reduced angle-dependence compared to the conventional B-mode (0°) image. When comparing the ultrasound images to the corresponding anatomical image, it was observed that the MACI image features a better definition of outlines and a more uniform representation of tissue parameters, compared to conventional B-mode imaging. Therefore, MACI is believed to have potential for improving diagnosis of atherosclerotic disease.

Acknowledgements

CADUS is supported by the Danish Technical and Medical Research Councils. The authors gratefully acknowledge the help by MD M.-L. Moes Grønholdt for providing the specimens and the help by instrument maker K. Martinsen for making the fixtures for the transducer and the biological specimens.

References

[1] European Carotid Surgery Trialist' Collaborative Group (ECST). Randomized trial of endarterectomy for recently symptomatic carotid stenosis: final results of the MRC European Carotid Surgery Trial (ECST). The Lancet, Vol. 351, pp. 1379-1387, 1998.

[2] Jespersen SK: Tools for improving the diagnosis of atherosclerotic plaque using ultrasound. PhD thesis. CADUS, Department of Information Technology, Technical University of Denmark, 1997.

[3] Jespersen SK, Wilhjelm JE, Sillesen H: Multi-angle compound imaging. Ultrasonic Imaging, Vol. 20, pp. 81-102. 1998.

[4] Picano E, Landini L, Distante A, Salvadori M, Lattanzi F, Masini M, L'Abbate A: Angle dependence of ultrasonic backscatter in arterial tissues: a study in vitro. Circulation, Vol. 72, No. 3, pp. 572-576, 1985.

[5] Shankar PM, Newhouse VL: Speckle Reduction with Improved Resolution in Ultrasound Images. IEEE Transactions on Sonics and Ultrasonics, Vol. 32, No. 4, pp. 537-543. 1985.

[6] Shattuck DP, Ramm OTv: Compound Scanning with a Phased Array. Ultrasonic Imaging, Vol. 4, pp. 93-107. 1982.

[7] Trahey GE, Smith SW, Ramm OTv: Speckle Pattern Correlation with Lateral Aperture Translation: Experimental Results and Implications for Spatial Compounding. IEEE Transactions on UFFC, Vol. 33, No. 3, pp. 257-264. 1986.

This paper was published simultaneously in "Technical Report of the Institute of Electronics, Information and Communication Engineers, US99-53, pp. 9-14, 1999".